

Weak Interaction Induces an ON/OFF Switch, whereas Strong Interaction Causes Gradual Change: Folding Transition of a Long Duplex DNA Chain by Poly-L-lysine

Tatsuo Akitaya,^{†,||} Asako Seno,[‡] Tonau Nakai,[†] Norio Hazemoto,[‡] Shizuaki Murata,[§] and Kenichi Yoshikawa^{*,†,⊥}

Department of Physics, Graduate School of Science, Kyoto University, Kyoto 606-8502, Japan, Faculty of Pharmaceutical Science, Nagoya City University, 3-1, Tanabedori, Mizuho-ku, Nagoya 467-8603, Japan, and Graduate School of Environmental Studies, Nagoya University, Furo-cho, Chikusa-ku, Nagoya 464-8601, Japan

Received July 1, 2006; Revised Manuscript Received August 12, 2006

A large-scale conformational change in genomic DNA is an essential feature of gene activation in living cells. Considerable effort has been applied to explain the mechanism in terms of key–lock interaction between sequence-specific regulatory proteins and DNA, in addition to the modification of DNA and histones such as methylation and acetylation. However, it is still unclear whether these mechanisms can explain the ON/OFF switching of a large number of genes that accompanies differentiation, carcinogenesis, etc. In this study, using single-molecule observation of DNA molecules by fluorescence microscopy with the addition of poly-L-lysine with different numbers of monomer units ($n = 3, 5, 9$, and 92), we found that an ON/OFF discrete transition in the higher-order structure of long duplex DNA is induced by short poly-L-lysine, whereas a continuous gradual change is induced by long poly-L-lysine. On the other hand, polycations with a lower positive charge have less potential to induce DNA compaction. Such a drastic difference in the conformational transition of a giant DNA between short and large oligomers is discussed in relation to the mechanisms of gene regulation in a living cell.

Introduction

Large-scale morphological changes in genomic DNA molecules between a compact state and loose state are closely related to gene activation, such as transcription and replication, in living cells. This process often occurs over the range of several tens of kilo base pairs of DNA in an all-or-none manner, concomitant with the cooperative transcription of large numbers of genes.^{1,2} Transcriptional silencing associated with dense methylation also occurs in large-scale genomic DNA in an all-or-none manner, with a dynamic change in the conformation, such as the chromatin structure.^{3,4} Many studies have been performed to explain transcriptional action at a distance based on sequence-specific, that is, key–lock, interaction between protein and DNA, and have proposed several models in which two proteins separate from each other can contact on a duplex DNA chain.^{5–8} However, the distance between these two key–lock protein-binding sites is at most hundreds or a few thousand base pairs of DNA, which can only involve one or a few genes,^{9–11} while a double-stranded DNA chain with a size larger than several thousand base pairs shows a change in conformation in an all-or-none manner during transcription. Moreover, there is little information available to precisely explain how a typical all-or-none conformational change in DNA molecules can occur even if proteins can cooperatively bind over a long range in a DNA molecule.

Regarding the large-scale conformational change in DNA molecules, there have been extensive in vitro studies on ion condensation in the vicinity of DNA molecules. There have been many findings on the effects of multivalent cations on DNA with regard to the binding equilibrium,^{12–14} kinetics,^{15,16} condensation/aggregation,^{15–27} and morphology of the binding complex.^{18,20,22} Up to the mid-1990s, studies on DNA condensation^{15–27} were performed with regard to the behavior of multiple DNA molecules, or with phenomena involving both single and multiple molecules. These studies have led to the general concept that DNA condensation is a steep but continuous process. Through the careful observation of DNA condensation at dilute DNA concentrations, Widom and Baldwin²⁸ concluded that (1) the transition is not a two-state reaction and (2) the transition for monomolecular condensation is diffuse through careful measurement with light-scattering. It is now clear²⁹ that this conclusion is attributable to the nature of the transition in the ensemble of DNA molecules; current methodologies such as light-scattering cannot distinguish between “intra”-molecular collapse and “inter”-molecular aggregation processes because of the principle of detecting signals averaged over the ensemble of DNA molecules.

We have recently established, with single-molecule observation by fluorescent microscopy, that individual giant DNA chains exhibit a large discrete transition, or ON/OFF switching, between elongated unfolded and compact folded states,³⁰ depending on the concentrations of various kinds of condensation agents, such as polyamines with three or four positive charges,²⁹ multivalent metal cations,³¹ nonionic surfactants,³² hydrophilic neutral polymers,³³ and cationic surfactants.³⁴ Such a folding transition typically takes place on duplex DNA that is sufficiently longer³⁰ than the persistent length of about 50

* To whom correspondence should be addressed. Phone: +81-75-753-3812. Fax: +81-75-753-3779. E-mail: yoshikaw@scphys.kyoto-u.ac.jp.

[†] Kyoto University.

^{||} Present address: Faculty of Pharmacy, Meijo University, 150 Yagotoyama, Tenpaku-ku, Nagoya 468-8503, Japan.

[‡] Nagoya City University.

[§] Nagoya University.

[⊥] Spatio-Temporal Order Project, ICORP, JST.

nm, that is, 150 base pairs. Based on theoretical considerations²⁹ with regard to statistical thermodynamics in the folding/unfolding transition induced by multivalent cations and the measured electrophoretic mobility of DNA,³⁵ it has been concluded that ion-exchange between univalent and multivalent ions plays an important role in stabilizing the folded compact state in single DNA molecules. The binding energy of a single multivalent ion ($3+$ or $4+$) with DNA chain is relatively small, on the order of $\sim kT$, that is, a weak interaction. This is in large contrast to the usual sequence-specific key–lock interaction, that is, a strong interaction. In this study, we investigated the effect of specificity in the interaction between long duplex DNA, T4 bacteriophage genome DNA, and poly-L-lysine of various lengths, that is, multivalent cations that differ with regard to the strength and specificity of binding to duplex DNA chain, to understand the origin of the ON/OFF switching in gene activation. We found that ON/OFF switching of the conformational change of DNA could not be induced by strong interaction with long poly-L-lysine but could be induced by weak, nonspecific interaction with short poly-L-lysine.

Experimental Section

Materials. T4 phage DNA composed of 166 kbp with a contour length of $57\ \mu\text{m}$ was purchased from Nippon Gene Co., Ltd. (Toyama, Japan) and used for fluorescence microscopy. Trimer, 92-mer, and 981-mer poly-L-lysine were from Sigma (St. Louis, MO). Pentamer poly-L-lysine was from Bachem AG (Bubendorf, Switzerland). Nona-mer poly-L-lysine was synthesized according to the fluoren-9-yl methoxycarbonyl (Fmoc) procedure³⁶ using a peptide synthesizer (model 431A, Applied Biosystems, Foster City, CA). Monomeric amino acids were purchased from Novabiochem (Darmstadt, Germany). To visualize DNA, 4',6-diamidino-2-phenylindole dihydrochloride (DAPI) was purchased from Wako Pure Chemicals Industries, Ltd. (Osaka, Japan).

Fluorescence Microscopy. The large-scale structure of T4 phage DNA with poly-L-lysine in aqueous solution was directly observed by fluorescence microscopy. To stain DNA molecules, DAPI was dissolved in DNA solution ($0.2\ \mu\text{M}$ in phosphate) to give a final concentration of $0.1\ \mu\text{M}$. It has been previously confirmed that the presence of DAPI at this concentration has no significant effect on the persistent length³⁷ or higher-order conformational change of DNA.³⁸ In addition, under this ultradilute condition of DNA, there is almost no chance for the DNA molecules to collide with each other during the observation period of several minutes. DAPI molecules in the sample solutions were excited by UV light (345 nm), and fluorescence images of DNA were observed at room temperature using a Carl Zeiss Axiovert 200M microscope.

Sample solution was situated between two thin glass plates (Matsumi No. 1, thickness: $120\text{--}170\ \mu\text{m}$) at a depth of $\sim 150\ \mu\text{m}$ using spacer glass plates. Because T4 DNA molecules have a mean size of less than $5\ \mu\text{m}$, many DNA molecules remained in the bulk solution during the observation period. Fluorescence images were recorded on videotape through a high-sensitivity Hamamatsu SIT TV camera and an Argus 10 image processor (Hamamatsu Photonics, Hamamatsu, Japan). The long-axis length was measured on 50–100 randomly selected DNA molecules under fixed conditions, where long-axis length is defined as the longest distance in the fluorescence image by using the image analysis software Cosmos 32 (Library, Tokyo, Japan). For observation, an aliquot of each sample solution was loaded on a chamber composed of glass slips, which were cleaned very carefully (burned at $500\ ^\circ\text{C}$ for 1 h). Because of the blurring effect of fluorescence light, the apparent size in DNA images is about $0.6\ \mu\text{m}$ larger than that of the actual DNA.³⁴

Imaging by Atomic Force Microscopy (AFM). A DNA solution containing poly-L-lysine was prepared as described above, and $5\ \mu\text{L}$ was adsorbed onto freshly cleaved mica for 1 min. The mica surface

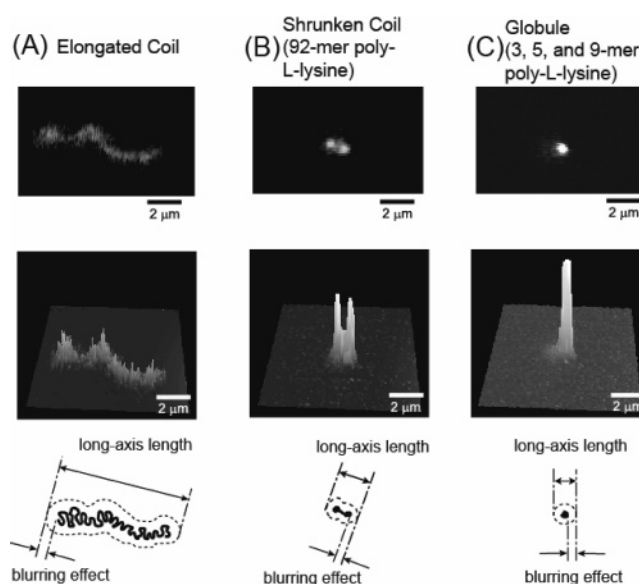


Figure 1. Top: Fluorescence images of single T4 DNA molecules in the presence of poly-L-lysine. (A) Elongated coil without poly-L-lysine, (B) shrunken coil induced by 92-mer poly-L-lysine in 0.25 [amino acid/phosphate], and (C) compact globule induced by 3-mer poly-L-lysine in 1.0×10^5 [amino acid/phosphate] in aqueous solution were observed under a microscope. Middle: Quasi-three-dimensional representations of the fluorescent light intensities of (A), (B), and (C). Bottom: Schematic representation of the relationship between the conformation of the actual DNA chain and the corresponding fluorescence images in the top column. Because of the blurring effect ($\sim 0.3\ \mu\text{m}$),³² the fluorescence image is larger than the actual size of the DNA chain.

was washed with Milli-Q-purified water and dried in N_2 gas. An NVB 100 (Olympus, Tokyo, Japan) operated in tapping mode was used. Images were displayed without modification except for flattening to remove the background curvature of the mica surface. Fluorescence images were taken first for a single molecule in solution with a fluorescent microscope joined with AFM, and then AFM scans were undertaken on the same sample after the single molecule gently adsorbed on the mica surface and the sample solution was dried.

Results

A folding transition typically takes place on duplex DNA that is sufficiently longer³⁰ than the persistent length³⁷ of about $50\ \text{nm}$, that is, $150\ \text{bp}$. A duplex DNA molecule longer than several tens of kbp is large enough for microscopic observation of single-molecule structure. In this study, we examined the effects of the length and concentration of poly-L-lysine on the higher-order structure of single T4 bacteriophage DNA ($166\ \text{kbp}$) molecules in buffer solution. The long-axis length, defined as the longest distance within the fluorescence images of DNA chains in a two-dimensional plane, was observed.

Figure 1 (top row) shows fluorescence microscopic images of individual T4 DNA molecules in aqueous solution in the absence and presence of poly-L-lysine. The middle row shows quasi-three-dimensional representations of the fluorescent light intensity distributions corresponding to the microscopic images in the top row. The bottom row shows schematic diagrams of individual DNA molecules, where the long-axis length is defined. Depending on the concentration of poly-L-lysine, DNA molecules exhibited intrachain and translational Brownian motion with different conformations. Without poly-L-lysine (Figure 1A), DNA molecules exhibit an elongated or swollen

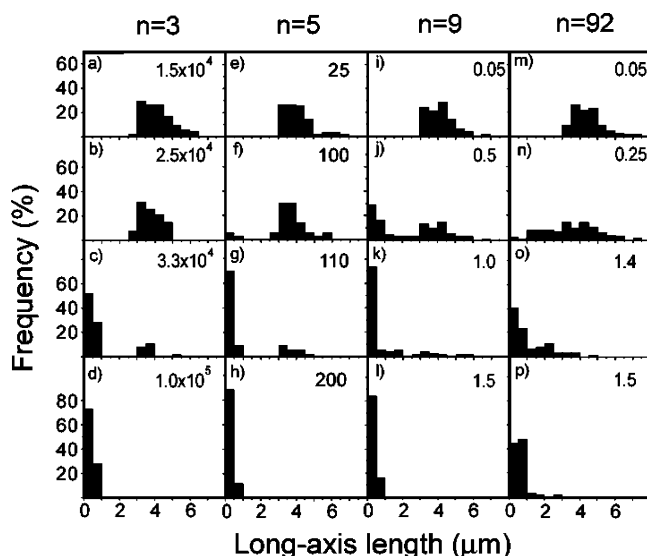


Figure 2. Classification of the higher-order structure of DNA molecules induced by linear poly-L-lysine. Each column shows the distribution of the average long-axis length of T4 DNA molecules in the aqueous phase under various concentrations of poly-L-lysine. The numbers at the top of each column and in each box indicate the number of amino acid residues and the charge ratios of poly-L-lysine and T4 DNA [amino acid/phosphate], respectively. T4 DNA used was 0.2 μ M in phosphate. In contrast to 3-, 5-, and 9-mer lysine, which show a substantially bimodal distribution of long-axis length, 92-mer L-lysine shows a continuous shift with a single distribution.

conformation. DNA molecules remain in an elongated structure at a low concentration for all of the types of poly-L-lysine used in the experiment. On the other hand, small spherical structures with intensive fluorescence (Figure 1C) predominantly appeared with a higher concentration of poly-L-lysine. There was a large difference in the nature of the Brownian motion of DNA molecules in the liquid phase between the diffused and spherical globule states. The elongated DNA molecules exhibited relatively slow translational fluctuation along with marked interchain thermal motion. In contrast, compact DNA showed significant translational motion without apparent intrachain fluctuation. Previous studies have suggested that the swollen and small compact structure corresponded to the elongated coil and compacted globule structures of single DNA molecules, respectively.²⁹ In contrast to DNA molecules with 3-, 5-, and 9-mer poly-L-lysine, which show a discrete change between elongated coil and compacted globule structures through a region in which both structures coexist, DNA molecules with 92-mer poly-L-lysine exhibited a shrunken coil structure (Figure 1B) that was intermediate between the elongated coil and compacted globule structures.

Figure 2 shows histograms of the long-axis length of T4 DNA molecules with poly-L-lysine of 3-, 5-, 9-, and 92-mer at various concentrations as described with each histogram. Representative conditions were chosen to clarify the boundaries of regions in which the long-axis length changes. With 3-mer (a, b, c, d), 5-mer (e, f, g, h), and 9-mer (i, j, k, l) poly-L-lysine, the distributions showed bimodal peaks at a long-axis length of about 4 μ m, corresponding to the elongated coil structure (Figure 1A), which is predominant under a low concentration of poly-L-lysine, and of less than 1 μ m, corresponding to the compact globule structure (Figure 1C), which is predominant under a higher concentration of poly-L-lysine. These distributions also showed a region of coexistence (b, c, f, g, j) of the coil and globule structures, although there are only a small number of intermediate-sized diffused DNA molecules (j, k) with 9-mer poly-L-lysine. In contrast, 92-mer poly-L-lysine exhibited a

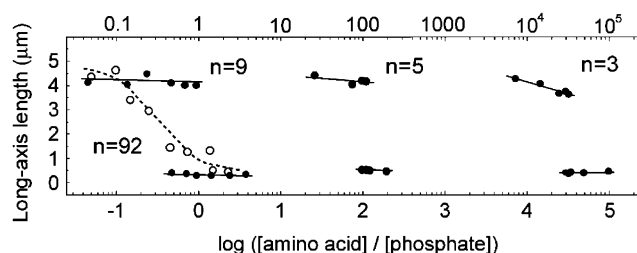


Figure 3. Change in the long-axis length as a function of the poly-L-lysine concentration. The horizontal axis shows the charge ratio between poly-L-lysine (amino group) and T4 (phosphate). The numbers n in each picture correspond to the number of residues in the poly-L-lysine molecule. Open and closed circles indicate the data of $n = 92$ and $n = 3, 5, 9$, respectively. Open circle represents the average for all DNA molecules in the given condition. Values shown with closed circles represents the average for coiled state and globular state individually. The concentration of T4 DNA used for all measurements is 0.2 μ M in phosphate.

unimodal distribution and showed a continuous shift in the distribution peak (m, n, o, p) according to the change in the poly-L-lysine concentration, consistent with a continuous change in the long-axis length of DNA molecules.

Figure 3 shows the average long-axis length in fluorescence images of individual DNA molecules in the liquid phase, observed under a microscope as a function of the concentration of 3-, 5-, 9-, and 92-mer linear poly-L-lysine. The numbers n shown in the figure correspond to the monomer number of each linear poly-L-lysine. With 3-, 5-, and 9-mer poly-L-lysine, the average long-axis length of DNA molecules showed a discrete transition, corresponding to the coexistence state in Figure 2, with charge ratios on the order of 10^4 , 10^2 , and 10^{-1} [amino acid/phosphate], respectively. DNA molecules observed below the charge ratio in the region of the discrete transition predominantly exhibited coil structures (Figure 1A), while globule structures (Figure 1C) were predominantly seen above the charge ratio in the region of the discrete transition. In the case of 9-mer, a small number of intermediate-sized coil DNAs were observed, and these coexisted with typical elongated coil and compact globular DNA molecules, as seen with 3- and 5-mer poly-L-lysine. In contrast to 3-, 5-, and 9-mer poly-L-lysine, 92-mer (O) poly-L-lysine induced a gradual continuous decrease in the average long-axis length with an increase in the charge ratio, and this was almost complete at a charge ratio of around 1.0 [amino acid/phosphate]. This gradual change coincided with a continuous decrease in the long-axis length of individual DNA molecules in the elongated coil state (Figure 1B) and was complete at a ratio of below around 1.0 [amino acid/phosphate] to form the folded globule structure. Almost the same profile was observed with longer, that is, 981-mer, poly-L-lysine (data not shown). Interestingly, this is consistent with the fact that the mixing ratio for compaction between positive and negative charges was 1 or less only when longer polycations were used in the interaction between DNA and positive agents.³⁹ The globule structure that appeared with 92-mer poly-L-lysine tended to form intermolecular aggregates and precipitate on the glass surface faster than that induced by short polyamine, which exhibited a repulsive interaction.³³ Additionally, globules induced by 92-mer poly-L-lysine were larger than the compact globules induced by 3-, 5-, and 9-mer poly-L-lysine, indicating that the globule formed with 92-mer poly-L-lysine is looser than that with short poly-L-lysine. There was also a marked difference in the concentration, that is, the affinity for DNA, of poly-L-lysine required to complete globule formation between short (3-, 5-, and 9-mer) and long 92-mer poly-L-lysine.

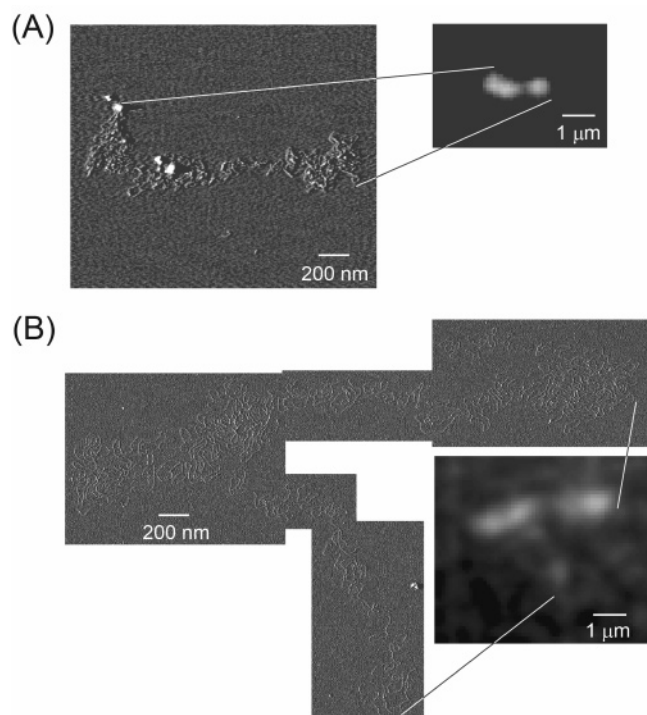


Figure 4. AFM and fluorescence microscopic images of T4 DNA molecules in the presence of poly-L-lysine. AFM images (left) and the corresponding fluorescence microscopic images (right) of (A) intermediate-sized shrunken coil T4 DNA molecule in the presence of 981-mer poly-L-lysine with a charge ratio of 0.2 [amino acid/phosphate], and (B) elongated coil T4 DNA molecule without poly-L-lysine, adsorbed on a mica surface. Fluorescence images were taken first for a single molecule in solution with a fluorescent microscope joined with AFM, and then AFM scans were undertaken on the same sample after the single molecule gently adsorbed on mica surface and the sample solution was dried. Each AFM image assembled in (B) was individually scanned to obtain high magnification.

Consequently, these results clearly show that 3-, 5-, and 9-mer poly-L-lysine interacted weakly with DNA and then induced a discrete, all-or-none-type change in the higher-order structure of DNA, while 92-mer poly-L-lysine interacted strongly and produced a gradual change.

Figure 4 shows the detailed morphological features of T4 DNA molecules observed by AFM and fluorescence microscopic images of exactly the same T4 DNA molecule on a mica surface in the (A) presence and (B) absence of 981-mer poly-L-lysine with a charge ratio of 0.2 [amino acid/phosphate]. With 981-mer poly-L-lysine, intrachain aggregations are observed with much higher resolution than those observed by fluorescence microscopy, as shown in (A), in contrast to the diffused coil structure shown in (B). It is clear that DNA strands randomly adhere to each other and relatively condensed parts assume a loosely packed conformation. This AFM picture corresponds well to the intermediate-sized shrunken coil structure observed by fluorescence microscopy with a lower resolution (Figures 1B and 4B), suggesting a marked difference from the intramolecular phase segregation observed in the discrete folding transition.³⁹

The present results constitute direct evidence that the ON/OFF change in the higher-order structure of DNA can be induced by sequence nonspecific and weak interaction with short poly-L-lysine, but not by strong interaction with long poly-L-lysine.

Discussion

We have shown that 9-mer or shorter poly-L-lysine induces an ON/OFF conformational transition of DNA, whereas 92-mer

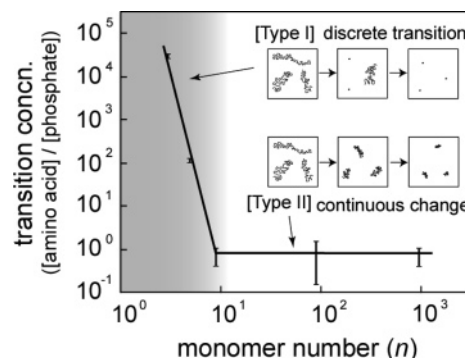


Figure 5. Transition concentration versus monomer number, n , of poly-L-lysine. Charge ratios of poly-L-lysine to T4 DNA ([amino acid]/[phosphate]) corresponding to the conformational change in DNA molecules are depicted as a function of the monomer number (n) of each poly-L-lysine. Vertical bars indicate regions in which coil and globule coexist for discrete transition or shrunken coil-structures were observed for continuous change.

lysine induces a gradual conformational change. Now let us discuss the mechanism of DNA compaction. Figure 5 shows the transition concentration as a function of the monomer number n . It is clear that the transition concentration varies differently between $n < 9$ and $n > 9$, which we call “Type I” and “Type II”, respectively; in the case of Type I, the transition concentration decreases 1 order of magnitude with an increase in n , whereas in the case of Type II, it is constant regardless of n . Furthermore, 3- and 5-mer poly-L-lysine exhibit a binding equilibrium where the dissociated state is predominant as compared to the bound state, contrary to 9- and 92-mer, considering that charge neutralization is necessary to induce DNA compaction. Concerning the mechanism of transition in the case of Type I, previous study revealed that transition occurs through two stages, the first attributed to cation binding and the second to DNA compaction.⁴⁰ Furthermore, in the second stage, as pointed out by Makita and Yoshikawa,⁴¹ DNA chains in the coexistence region can be considered to be in a kind of equilibrium between the elongated and compact states, and a large excess of cations, that is, sufficient gain in translational entropy, is necessary to induce compaction. According to previous studies, such a conformational transition is discrete.^{29–35} In contrast, longer, that is, multiply charged, poly-L-lysine can bind rather strongly to DNA and tends to adhere DNA chains to each other, which promotes bridging between different sites in the DNA chain. Thus, we can guess that the condensation occurs gradually and is completed before the charge is neutralized (Figure 6, bottom). In this situation, the folded globule structure formed upon the addition of poly-L-lysine seems to be rather swollen, that is, lower in density as described in the probability distribution profiles in Figure 6, and may contain remaining electrical charges that cause intramolecular segregation, as observed with longer poly-L-lysine (Figure 1, center and Figure 4, top). Tang et al. found that even with long poly-L-lysine DNA can take a compact toroidal form.⁴² We think this conformational difference is attributed to the kinetic pathway; in their study, DNA and poly-L-lysine are repeatedly mixed with a micropipet and vortex mixer and then incubated, while in the present study, poly-L-lysine was gently dissolved in the DNA solution and immediately observed. Moreover, the lengths of DNA used are quite different between their study and the present study. Thus, we consider that the shrunken structure obtained in this study is attributed to the kinetic effect.

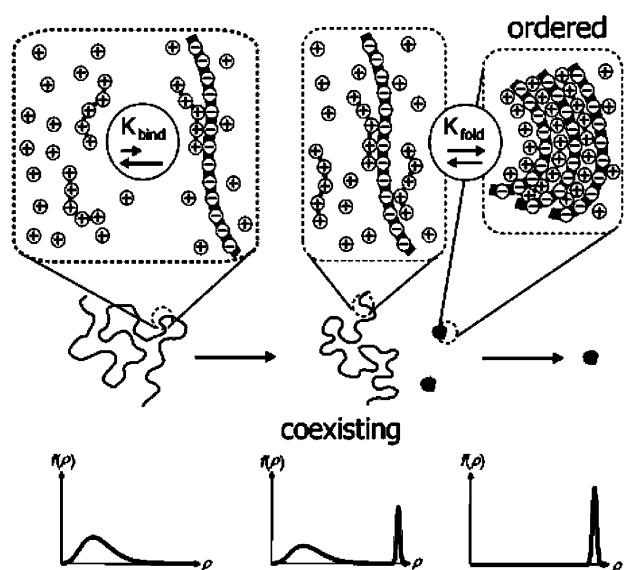
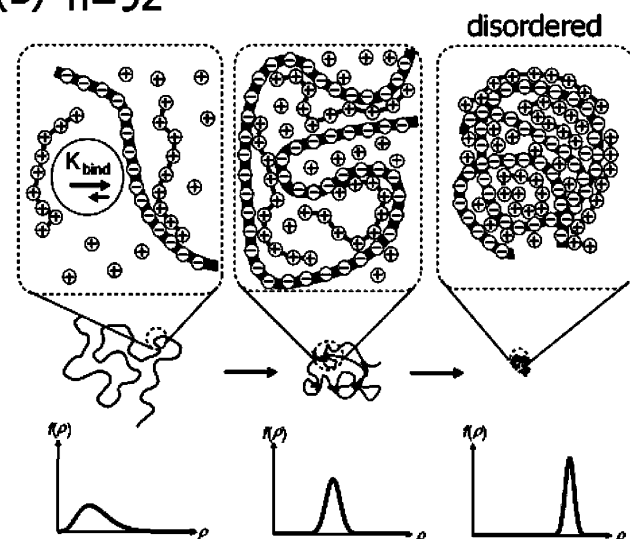
(A) $n=3, 5, 9$ (B) $n=92$ 

Figure 6. Schematic representation of two types of folding for DNA molecules with the addition of shorter (top) and longer (bottom) poly-L-lysine. The numbers n indicate the number of residues in a poly-L-lysine molecule. K_{bind} is the binding constant of poly-L-lysine to phosphate groups in an elongated DNA chain. K_{fold} represents the equilibrium constant between the elongated coil and compact globular states of DNA, where the manner of binding of poly-L-lysine changes drastically. Diagrams below each scheme show the probability distribution profile of DNA molecules as a function of density (ρ) of individual DNA molecules corresponding to the states shown in the schemes. The density of folded globule structure formed with longer (top) poly-L-lysine seems to be lower than that with shorter (bottom) poly-L-lysine.

Consequently, we can depict schematically, as shown in Figure 6, the difference in the manner of the change in the higher-order structure of DNA dependent on the length of poly-L-lysine molecules.

Gene activation essentially occurs in an all-or-none, that is, ON/OFF, manner over the range of several tens of base pairs of DNA molecule,^{1,2} concomitant with the spontaneous expression of abundant genes.² It is generally considered that proteins play major roles in transcription at a distance on a long DNA molecule "sequence-specifically", that is, strongly, bound to DNA, like transcription factors.⁴³ Several models have been

proposed to explain this action on a long duplex DNA chain:^{5–8} (1) loop formation in a DNA chain to move two separate DNA-binding proteins adjacent to each other, (2) sliding of a protein along a DNA chain to the vicinity of another protein, (3) cooperative protein binding onto a DNA chain where the binding of one protein aids in the binding of another protein to the adjacent site, and (4) a local distortion in the conformation of DNA induced by protein binding and subsequent propagation along the DNA chain to another protein-binding site. These models enable two proteins that are sequence-specifically bound to DNA to contact each other at a distance. However, it is also known that the distance between these two protein-binding sites can reach at most hundreds or a few thousand base pairs of DNA where only one or a few genes can be involved, although more than several thousand base pairs of DNA change the conformation in an all-or-none manner during transcription. Moreover, there is little clear evidence to exactly explain the typical all-or-none change in the conformation of DNA molecules. It has generally been speculated that the large-scale bimodal nature of gene activation may be due to cooperative multisite binding between proteins and DNA.^{44,45} However, there has been neither clear experimental evidence nor theoretical support for this proposition. Moreover, it has also been shown that highly concentration-sensitive mechanisms such as multisite binding become unrealistic in the intracellular environment where dramatic thermal fluctuation occurs.⁴⁶ Although previous reports have described apparently contradictory correlations between DNA conformations and biochemical reactivity, the higher-order structure of DNA must be considered one of the most important factors in gene regulation.^{22,47,48} We have demonstrated here that ON/OFF switching of the higher-order structure of DNA cannot be induced by strong, that is, sequence-specific interaction, but can be induced by weak, nonspecific, interaction between ligands and DNA. Bork and Copley⁴⁹ suggested that the cellular environment and genome packing might contribute to the regulation of gene expression. In fact, *in vitro* studies have reported that environmental chemical species such as polyamines and NTPs induce ON/OFF switching in the action of restriction endonuclease⁵⁰ and transcriptional activity.^{46,51} It is highly expected that chemical species in the environment such as ATP, RNA, potassium, and chloride can strongly affect the higher-order structure of DNA and that gene activation through a scenario similar to the effect of weak and sequence-nonspecific interaction with DNA. Thus, our conclusion leads to the hypothesis that gene activation may be regulated by intracellular environmental chemical species through weak sequence-nonspecific interaction with DNA, in addition to the previously known mechanism of gene activation through sequence-specific, that is, key–lock, interaction between regulatory protein and DNA. This proposes a hierarchical gene activation mechanism that arises through weak sequence-nonspecific interaction by cytoplasmic environmental chemical species through large-scale ON/OFF switching of the higher-order structure of DNA, in addition to local gene activation by sequence-specific regulatory proteins.

Supporting Information Available. We thank Dr. Michiko Ito (Department of Materials and Environment, Division of Environmental Engineering and Architecture, Graduate School of Environmental Studies, Nagoya University, Nagoya, Japan) for the gift of poly-L-lysine and for helpful discussions, Dr. Naoko Makita for providing helpful discussions and suggestions, and Ms. Eri Shindo for her helpful support in the experiment. This work was partly supported by a Grant-in-Aid for Creative Scientific Research (No. 18GS0421) from the Japan Society

for the Promotion of Science (JSPS) and by a Grant-in-Aid on Priority Areas (No. 17076007) from the Ministry of Education, Culture, Sports, Science, and Technology of Japan.

References and Notes

- (1) Rutter, J.; Reick, M.; Wu, L. C.; McKnight, S. L. *Science* **2001**, 293, 510–514.
- (2) Ueda, H. R.; Chen, W.; Adachi, A.; Wakamatsu, H.; Hayashi, S.; Takasugi, T.; Nagano, M.; Nakahama, K.-i.; Suzuki, Y.; Sugano, S.; Iino, M.; Shigeyoshi, Y.; Hashimoto, S. *Nature* **2002**, 418, 534–539.
- (3) Mizutani, T.; Ito, T.; Nishina, M.; Yamamichi, N.; Watanabe, A.; Iba, H. *J. Biol. Chem.* **2002**, 277, 15859–15864.
- (4) Lorincz, M. C.; Dickerson, D. R.; Schmitt, M.; Groudine, M. *Nat. Struct. Mol. Biol.* **2004**, 11, 1068–1075.
- (5) Ptashne, M. *Nature* **1986**, 322, 697–701.
- (6) Wang, J. C.; Giaever, G. N. *Science* **1988**, 240, 300–304.
- (7) Adzuma, K.; Mizuuchi, K. *Cell* **1989**, 57, 41–47.
- (8) Hochschild, A. *Methods Enzymol.* **1991**, 208, 343–341.
- (9) Dandanell, G.; Valentin-Hansen, P.; Larsen, J. E. L.; Hammer, K. *Nature* **1987**, 325, 823–826.
- (10) Miller, J. A.; Widom, J. *Mol. Cell Biol.* **2003**, 23, 1623–1632.
- (11) Cook, P. R. *J. Cell Sci.* **2003**, 116, 4483–4491.
- (12) Braunlin, W. H.; Strick, T. J.; Record, M. T., Jr. *Biopolymers* **1982**, 21, 1301–1314.
- (13) Igarashi, K.; Sakamoto, I.; Goto, N.; Kashiwagi, K.; Honma, R.; Hirose, S. *Arch. Biochem. Biophys.* **1982**, 219, 438–443.
- (14) Rowatt, E.; Williams, R. J. P. *J. Inorg. Biochem.* **1992**, 46, 87–97.
- (15) Porschke, D. *Biochemistry* **1984**, 23, 4821–4828.
- (16) Bloomfield, V. A. *Biopolymers* **1997**, 44, 269–282.
- (17) Gosule, L. C.; Schellman, J. A. *J. Mol. Biol.* **1978**, 121, 311–326.
- (18) Chatteraj, D. K.; Gosule, L. C.; Schellman, J. A. *J. Mol. Biol.* **1978**, 121, 327–337.
- (19) Wilson, R. W.; Bloomfield, V. A. *Biochemistry* **1979**, 18, 2192–2196.
- (20) Allison, S. A.; Herr, J. C.; Schurr, J. M. *Biopolymers* **1981**, 20, 469–488.
- (21) Thomas, T. J.; Bloomfield, V. A. *Biopolymers* **1983**, 22, 1097–1106.
- (22) Baeza, I.; Gariglio, P.; Rangel, L. M.; Chavez, P.; Cervantes, L.; Arguello, C.; Wong, C.; Montañez, C. *Biochemistry* **1987**, 26, 6387–6392.
- (23) Raspaud, E.; Olvera de la Cruz, M.; Sikorav, J.-L.; Livolant, F. *Biophys. J.* **1998**, 74, 381–393.
- (24) Saminathan, M.; Antony, T.; Shirahata, A.; Sigal, L. H.; Thomas, T.; Thomas, T. J. *Biochemistry* **1999**, 38, 3821–3830.
- (25) Raspaud, E.; Chaperon, I.; Leforestier, A.; Livolant, F. *Biophys. J.* **1999**, 77, 1547–1555.
- (26) Jary, D.; Sikorav, J.-L. *Biochemistry* **1999**, 38, 3223–3227.
- (27) Rodger, A.; Sanders, K. J.; Hannon, M. J.; Meistermann, I.; Parkinson, A.; Vidler, D. S.; Haworth, I. S. *Chirality* **2000**, 12, 221–236.
- (28) Widom, J.; Baldwin, R. L. *Biopolymers* **1983**, 22, 1595–1620.
- (29) Takahashi, M.; Yoshikawa, K.; Vasilevskaya, V. V.; Khokhlov, A. R. *J. Phys. Chem. B* **1997**, 101, 9396–9401.
- (30) Yoshikawa, K. *J. Biol. Phys.* **2002**, 28, 701–712.
- (31) Yamasaki, Y.; Yoshikawa, K. *J. Am. Chem. Soc.* **1997**, 119, 10573–10578.
- (32) Mel'nikov, S. M.; Yoshikawa, K. *Biochem. Biophys. Res. Commun.* **1997**, 230, 514–517.
- (33) Yoshikawa, Y.; Yoshikawa, K. *FEBS Lett.* **1995**, 361, 277–281.
- (34) Mel'nikov, S. M.; Sergeyev, V. G.; Yoshikawa, K. *J. Am. Chem. Soc.* **1995**, 117, 9951–9956.
- (35) Yamasaki, Y.; Teramoto, Y.; Yoshikawa, K. *Biophys. J.* **2001**, 80, 2823–2832.
- (36) Atherton, E.; Gait, M. J.; Sheppard, R. C.; Williams, B. J. *Bioorg. Chem.* **1979**, 8, 351–370.
- (37) Persistent length λ is defined as $\langle \cos(s) \rangle = \exp(-s/\lambda)$, where the magnitude $\langle \cos(s) \rangle$ is the mean cosine of the angle (s) between the chain segments separated by the length s on the polymer chain.⁵² Memory of chain direction is retained on length scales shorter than λ , but lost once λ is exceeded. Persistent length is a constant for each given polymer chain, for example, ca. 50 nm for duplex DNA in usual physiological solutions, and a basic characteristic of polymer flexibility.
- (38) Yoshinaga, N.; Akitaya, T.; Yoshikawa, K. *Biochem. Biophys. Res. Commun.* **2001**, 286, 264–267.
- (39) Kidoaki, S.; Yoshikawa, K. *Biophys. J.* **1996**, 71, 932–939.
- (40) Matulis, D.; Rouzina, I.; Bloomfield, V. A. *J. Mol. Biol.* **2000**, 296, 1053–1063.
- (41) Makita, N.; Yoshikawa, K. *Biophys. Chem.* **2002**, 99, 43–53.
- (42) Tang, M. X.; Li, W.; Szoka, F. C., Jr. *J. Gene Med.* **2005**, 7, 334–342.
- (43) Horikoshi, M.; Hai, T.; Lin, Y.-S.; Green, M. R.; Roeder, R. G. *Cell* **1988**, 54, 1033–1042.
- (44) Zhang, J.; Xu, F.; Hashimshony, T.; Keshet, I.; Cedar, H. *Nature* **2002**, 420, 198–202.
- (45) Adams, C. C.; Workman, J. L. *Mol. Cell. Biol.* **1995**, 15, 1405–1421.
- (46) Tsumoto, K.; Luckel, F.; Yoshikawa, K. *Biophys. Chem.* **2003**, 106, 23–29.
- (47) Krasnow, M. A.; Cozzarelli, N. R. *J. Biol. Chem.* **1982**, 257, 2687–2693.
- (48) Baeza, I.; Aguilar, L.; Santiago, R.; Ibanez, M.; Wong, C. *Rev. Latinoam. Microbiol.* **1997**, 39, 47–56.
- (49) Bork, P.; Copley, R. *Nature* **2001**, 409, 818–820.
- (50) Oana, H.; Tsumoto, K.; Yoshikawa, Y.; Yoshikawa, K. *FEBS Lett.* **2002**, 530, 143–146.
- (51) Akitaya, T.; Tsumoto, K.; Yamada, A.; Makita, N.; Kubo, K.; Yoshikawa, K. *Biomacromolecules* **2003**, 4, 1121–1125.
- (52) Grosberg, A. Yu.; Khokhlov, A. R. *Statistical Physics of Macromolecules*; AIP Press: New York, 1994.

BM06034J